

**A GIS-based fire spread simulator integrating a simplified physical wildland fire model and a wind field model**

Journal:	<i>International Journal of Geographical Information Science</i>
Manuscript ID	IJGIS-2016-0265.R3
Manuscript Type:	Research Article
Keywords:	GIS integration, ArcPy, Wildland fire spread model, Wind field model

SCHOLARONE™  
Manuscripts

*International Journal of Geographical Information Science*  
Vol. 00, No. 00, May 2017, 1–22

## RESEARCH ARTICLE

### A GIS-based fire spread simulator integrating a simplified physical wildland fire model and a wind field model

D. Prieto<sup>a,\*</sup>, M.I. Asensio<sup>a,b,\*</sup>, L. Ferragut<sup>a,b</sup>, J.M. Cascón<sup>b,c</sup> and A. Morillo<sup>d</sup>  
<sup>a</sup>*Applied Mathematics Department, University of Salamanca, Casas del Parque 2, 37008, Salamanca, Spain;*

<sup>b</sup>*Fundamental Physics and Mathematics University Institute, University of Salamanca, Casas del Parque 1, 37008, Salamanca, Spain;*

<sup>c</sup>*Economy and Economic History Department, University of Salamanca, Edificio FES, Campus Miguel de Unamuno, 37007, Salamanca, Spain;*

<sup>d</sup>*SEAGA, Xunta de Galicia, Pol. Ind. do Tambre, Vía Marconi, 14, 15890, Santiago de Compostela, Spain;*

*(v4.0 released May 2017)*

This article discusses the integration of two models, namely, the Physical Forest Fire Spread (PhFFS) and the High Definition Wind Model (HDWM), into a GIS-based interface. The resulting tool automates data acquisition, pre-processes spatial data, launches the aforementioned models, and displays the corresponding results in a unique environment. Our implementation uses the Python language and Esri's ArcPy library to extend the functionality of ArcMap 10.4. The PhFFS is a simplified 2D physical wildland fire spread model based on conservation equations, with convection and radiation as heat transfer mechanisms. It also includes some 3D effects. The HDWM arises from an asymptotic approximation of the Navier-Stokes equations, and provides a 3D wind velocity field in an air layer above the terrain surface. Both models can be run in standalone or coupled mode. Finally, the simulation of a real fire in Galicia (Spain) confirms that the tool developed is efficient and fully operational.

**Keywords:** GIS integration; ArcPy; Wildland fire spread model; Wind field model

---

\*Corresponding authors. Email: dpriher@usal.es, mas@usal.es

## 1. Introduction

According to the last available fire management global assessment from FAO (2007), the global estimate of land area affected by fire in 2000 was 350 million hectares, much of which was forest and woodland. Most of the area burned was in sub-Saharan Africa, followed at some distance by Australia. In more recent regional reports wildfire event data can be found, some of them as devastating as in Greece in August 2007, in all the Mediterranean countries in August 2009, in European Russia during the hot summer of 2010, in boreal forest of Alberta, Canada, in 2011 and again in 2016, and the most recent in Chile in January 2017. The intensity, frequency and duration of wildland fires are now considered to be directly influenced by global warming. Wildland fires are not only a result of a changing climate, however; they also emit greenhouse gases and therefore also contribute to global warming (Flannigan *et al.* 2009). Besides the huge environmental damage, wildland fires do not only bring about huge economical losses, they also cause human casualties. In brief, wildland fires have become one of the most pressing environmental, social and economic issues threatening the world's forests.

Therefore, the real-time simulation of wildland fire spread has direct applications in prevention (risk mapping, reforestation policies, and the design of fuelbreaks), in fire-fighting (predicting a fire's pathway helps to mobilise and optimise resources, improve firefighters' safety during extinguishing works, issue warnings, and evacuation planning), and in prescribed burn planning.

Numerous wildfire models have already been developed, and they can be classified into different types according to the nature of their construction: physical, semi-physical, or empirical (Pastor *et al.* 2003, Sullivan 2009a,b), although the nomenclature varies. Some authors argue that for a model to be classified as physical it must cater for both the physics and chemistry of the fire spread; semi-physical models are defined as those that seek to represent only the physics of the problem; and empirical models are those based on a phenomenological description or statistical regression of observed fire behaviour. According to the physical process modelled, wildland fire models can also be grouped as ground fires, surface fires, crown fires, and spotting models (Pastor *et al.* 2003). Since surface fires are the most predominant there exists an intensive research in this type of models.

The wildland fire model we propose is called Physical Forest Fire Spread-PhFFS (Asensio and Ferragut 2002, Ferragut *et al.* 2007a,b). It is a simplified 2D one-phase semi-physical model for surface fires based on the fundamental physics of combustion and fire spread, together with certain appropriate assumptions. The model considers two important forms of heat transfer in these kinds of fires, namely, convection and radiation (Anderson 1969), although their relative importance varies from fire to fire, and estimating their exact combination is not simple (Frankman *et al.* 2013, Finney *et al.* 2015). The model also takes into account the heat lost by natural convection, the effect of the flame tilt by wind or slope over the heat transfer and the influence of fuel moisture content and fuel type. The numerical solution of the model equations involves efficient numerical and computational tools for simulating a real scenario in less than real time.

One of the factors most influencing wildland fire spread is the wind (Viegas 2004). The PhFFS model can use meteorological wind data or be coupled with the High Definition Wind Model-HDWM (Asensio *et al.* 2005, Ferragut *et al.* 2011). This wind model arises from an asymptotic approximation of the Navier-Stokes equations, providing a 3D velocity wind field. It only requires meteorological wind measures at a small number of

1  
2  
3  
4 points in the simulation area, as well as information on surface topography and roughness.

5 Wildland fire simulation requires coupling spatial data with the simulation model. This  
6 approach calls for a spatial data management system to handle the diverse resources  
7 of information needed as input data for the wildland fire model, and for displaying  
8 the simulation results. The combination of environmental models and their spatial and  
9 temporal information using Geographical Information Systems (GIS) has been largely  
10 studied and applied (Skidmore 2002), as GIS allows building integrated database systems.  
11 Due to the spatial nature of the fire spread, GIS are widely used in wildland fire studies  
12 (Ager *et al.* 2011). The development of wildland fire risk maps with GIS (Chuvieco and  
13 Duarte 1996) is an example of one such application. The simulation of wildland fire  
14 spread is another important and common GIS application (Yassemi *et al.* 2008, Mandel  
15 *et al.* 2014, Williams *et al.* 2014). Currently several wildland fire spread models integrated  
16 in GIS are already being used, most of them are empirical mainly based on perimeter  
17 propagation. These models are very fast, but have many limitations, as they depend  
18 on a fire front spread rate that is generally empirically computed, in most cases by  
19 applying Rothermel's model (1972), so they are only applicable to situations in which  
20 the conditions are identical to those used in their formulation and adjustment. There  
21 are different types of perimeter propagation models: front-tracking methods, cellular  
22 methods and, more recently, level set methods (Hilton *et al.* 2015). An example of a  
23 wildfire growth model based upon front-tracking methods is FARSITE (Finney 2004),  
24 widely used in the US by federal and state land management agencies, based upon  
25 BEHAVE (Andrews 1986) fire behaviour prediction, which itself is an implementation  
26 of Rothermel's model, and produces outputs compatible with GIS software for later  
27 analysis and displays. Other examples are as follows: Prometheus (Tymstra *et al.* 2010),  
28 the Canadian Wildland Fire Growth Simulation Model, which exports simulated data  
29 for GIS systems; and SiroFire (Coleman and Sullivan 1996), the CSIRO Bushfire Spread  
30 Simulator developed for operational use in Australia that uses GIS-derived geographic  
31 maps and digital terrain models to graphically present the spread of the simulated fires.  
32 The models based upon cellular methods include FireStation (Lopes *et al.* 2002), which  
33 optionally imports the input data from GIS common formats, FIREMAP (Vasconcelos  
34 and Guertin 1992), which integrates the BEHAVE system and GIS using discrete event  
35 system specifications DEVS; and many others (Perry *et al.* 1999, Yassemi *et al.* 2008) also  
36 based on Rothermel's model. The more recent level-set method is the perimeter-growth  
37 approach used in the WRF-Fire model (Mandel *et al.* 2011), which couples the WRF  
38 atmosphere model and SFIRE fire spread model, again based on Rothermel's model, that  
39 has been recently integrated into a GIS (Mandel *et al.* 2014).

40  
41  
42 By contrast, physical or semi-physical models have not been so widely integrated  
43 into GIS tools due to their complexity and computational cost. One of the foremost  
44 physical wildland fire models is HIGRAD-FIRETEC (Linn *et al.* 2002), a physics-  
45 based, 3D computer code designed to simulate the interactive relationship between  
46 fire, fuels, atmosphere and topography, based on the FIRETEC fire model (Linn 1997)  
47 and the HIGRAD (Reisner *et al.* 1997) fluid-dynamics model. FIRETEC has a high  
48 computational cost, so it is presently a research tool only.

49 The novelty of this current work is that the wildland fire spread model integrated into  
50 GIS is a simplified physical model for faster-than-real-time simulation, that also includes  
51 its own wind velocity model. Both models can be compiled for any platform, and can  
52 operate either together or separately: the PhFFS model can operate with constant wind  
53 or with wind data provided by the HDWM or any other wind model. Furthermore, the  
54 HDWM model can provide wind field data from punctual meteorological data for other  
55  
56  
57  
58  
59  
60

1  
2  
3  
4 purposes. The scope of application of the GIS interface developed for these two models is  
5 initially Spain, but it can be extended to other countries by compiling the corresponding  
6 maps. Both models, PhFFS and HDWM, and their integration into the commercial suite  
7 ArcGIS Desktop 10.4 tool have been developed by the same research group, providing  
8 full control of the end product. The functionalities of Esri's software have been extended  
9 by an add-in to provide a flexible and user-friendly end-user interface for simulating a  
10 real fire and/or a wind field. This add-in permits the user to perform the pre-processing  
11 task in order to provide all the necessary data for the simulation. It also automates the  
12 input of temporal data, such as weather conditions, ignition points, or fire suppression  
13 tactics. In addition, our add-in can be used to launch the simulation and, finally, to  
14 load the results for their analysis and display on a basemap that is easily understood by  
15 non-specialist users. Furthermore, the accurate adjustment of both PhFFS and HDWM,  
16 is one of the current challenge of their development, and their GIS integration will enable  
17 this task to be handled more easily and improve the adjustment process.

18  
19 This paper is organized as follows: Section 2 reviews the physical models integrated  
20 into GIS software. Section 3 addresses the main issues in the process of developing the  
21 add-in for the ArcGIS software. Section 4 evaluates the resulting tool's performance by  
22 simulating a wildfire that occurred near Ourense (Spain) in September 2009, comparing  
23 the simulation results with the real fire's progress. Finally, the paper ends with its  
24 conclusions in Section 5.

## 27 2. The physical models

28  
29 This section briefly describes the underpinnings of the two models coupled with the  
30 GIS to provide the operational wildland fire simulation GIS-based tool: PhFFS and  
31 HDWM. Both models have been developed by the research group to which most of the  
32 authors belong, the Research Group of Numerical Simulation and Scientific Calculus of  
33 the University of Salamanca. We also outline both models input and output variables  
34 and parameters as a step towards their integration into a GIS.

### 37 2.1. PhFFS

38  
39 The Physical Forest Fire Spread (PhFFS) is the current version in a series of physical fire  
40 propagation models. It has its origin in a simple 2D one-phase physical model, based on  
41 the principles of energy and mass conservation, and considered convection and diffusion.  
42 In due course, heat transfer by radiation was incorporated into the model with a local  
43 radiation term (Asensio and Ferragut 2002). The influences of fuel moisture content and  
44 heat absorption by pyrolysis were included by Ferragut *et al.* (2007b) with an operator  
45 representing enthalpy. At the same time, the non-local radiation from the flames above  
46 the vegetal layer was added to the model (Ferragut *et al.* 2007a), enabling it to deal with  
47 the effect that wind and slope had over flame tilt and thus increasing heat transfer. Fresh  
48 efforts have been made to improve the suitability of the PhFFS model for the simulation  
49 of real fires in Ferragut *et al.* (2014) and experimental fires in Prieto *et al.* (2015), with  
50 the introduction of data assimilation techniques in Ferragut *et al.* (2015).

51  
52 The partial differential equations describing the PhFFS model are based on the energy  
53 and mass conservation equation on the surface where the fire takes place, and the  
54 radiation equation on the air layer over this surface. The model equations are not  
55 described here because of their mathematical complexity. A detailed explanation of the  
56  
57  
58  
59  
60

1  
2  
3  
4 current PhFFS model equations can be found in Prieto *et al.* (2015), although here we  
5 briefly describe the physical meaning of each of the equations terms. We also outline the  
6 equations unknowns, its input variables and its three parameters, that are summarised  
7 in Section 2.4, in order to understand how the PhFFS model is coupled with GIS.

8 The surface where the fire develops is given by a function  $h$  representing the  
9 topography; that is, the function  $h$  gives the land surface height.

10 The physical quantities involved as the unknowns in the model equations are enthalpy  
11  $E$  ( $J m^{-2}$ ), solid fuel temperature  $T$  ( $K$ ) and fuel load  $M$  ( $kg m^{-2}$ ). The following  
12 input variables are also required: the heat capacity of the solid fuel  $C$  ( $J K^{-1} kg^{-1}$ ), the  
13 maximum solid fuel load  $M_0$  ( $kg m^{-2}$ ), both depending on fuel type, and the reference  
14 temperature, which is the ambient temperature  $T_\infty$  ( $K$ ).

15 The influence of the vegetation's moisture content is modelled through an operator  
16 depending on enthalpy, the latent heat of evaporation  $\Lambda_v$  ( $J kg^{-1}$ ), and fuel moisture  
17 content  $M_v$  ( $kg$  of water/ $kg$  of dry fuel).

18 The model also takes into account the energy lost by natural free convection through a  
19 term in the energy conservation equation. This term is related to the natural convection  
20 coefficient  $H$  ( $J s^{-1} m^{-2} K^{-1}$ ), the first of the three model parameters.

21 Our model considers wind effect in two different ways: through the convective term  
22 itself and through the flame tilt caused by wind that affects the radiation term. The  
23 energy conservation equation incorporates a term representing convective heat. This term  
24 depends on the surface wind velocity,  $\mathbf{V}$  ( $m s^{-1}$ ), re-scaled by a correction factor  $\beta$ , which  
25 is the second model parameter. To deeply understand the meaning of this parameter  $\beta$   
26 see Prieto *et al.* (2015), where it is explained how this one solid phase model is simplified  
27 from a two phase solid-gas model, and how the assumptions of this simplification allow to  
28 estimate this parameter. Surface wind velocity  $\mathbf{V}$  is provided by meteorological sources.  
29 The HDWM (or any other wind model) is used to compute a 3D wind velocity field from  
30 these meteorological data. Then, the wind velocity at flame average weight is supplied  
31 as input data to PhFFS. Alternatively, surface wind velocity  $\mathbf{V}$  can be considered as  
32 constant wind along the simulation area.

33 The thermal radiation reaching the surface from the flame is included in the energy  
34 conservation equation, taking into account the influence of wind and slope over flame  
35 tilt. The radiation equation contains the third and final model parameter, the radiation  
36 absorption coefficient  $a$  ( $m^{-1}$ ), and two model variables, flame temperature denoted by  
37  $T_f$  ( $K$ ) and flame length  $F$  ( $m$ ), with both depending on fuel type. For further details  
38 about radiation computation see Ferragut *et al.* (2015).

39 An important simplification of the PhFFS model is that only the solid phase of  
40 the combustion process is considered: the solid fuel mass  $M$ , varies between 0 and its  
41 maximum value  $M_0$ , and the maximum value of solid fuel temperature  $T$  is the pyrolysis  
42 temperature  $T_p$  ( $K$ ). The gaseous phase is parameterized in the radiation term through  
43 flame temperature  $T_f$ , and flame length  $F$ .

44 The loss rate of solid fuel due to combustion is represented in the mass conservation  
45 equation. It is null when the pyrolysis temperature has not been reached, and constant  
46 once it has been exceeded. This constant value is inversely proportional to the solid fuel  
47 half-life of the combustion,  $t_{1/2}$  ( $s$ ), of each type of fuel, measured from the moment of  
48 ignition.

49 The numerical solution of the model is obtained by solving the corresponding non-  
50 dimensional partial differential equations depending on the non-dimensional solid fuel  
51 temperature  $u = \frac{T-T_\infty}{T_p-T_\infty}$ , and the non-dimensional solid fuel mass fraction  $c = \frac{M}{M_0}$ . The  
52 numerical methods used are the finite element method combined with various finite  
53  
54  
55  
56  
57  
58  
59  
60



1  
2  
3  
4 difference schemes in time, the characteristic method for the convective term, and an  
5 exact integration method assuming a rectangular flame shape section (under windy  
6 conditions we assume tilted flames) for the non-local radiation equation. With a view to  
7 reducing the computational cost of the 3D radiation equation, active nodes are defined  
8 for solving this equation only where necessary in the vicinity of the flames. These efficient  
9 numerical methods, together with different parallel computing techniques, ensure that  
10 the computational cost of running the PhFFS model has been significantly reduced,  
11 whereby it can compete with other simpler models.

12 The PhFFS model is implemented in C++, using API OpenMP (Chapman *et al.*  
13 2008) in order to exploit today's multiprocessor platforms for reducing computational  
14 time. This implementation is entered in the Spanish Registry of Intellectual Property on  
15 16 July 2015 under record entry 00/2015/4720.

## 18 2.2. HDWM

19 The origin of the High Definition Wind Model (HDWM) lies in an asymptotic  
20 approximation of the primitive Navier-Stokes equations considering that the horizontal  
21 dimensions are much larger than the vertical ones. The aim is to provide a 3D wind  
22 velocity field in the air layer over the surface of study, solving only 2D linear equations  
23 so that it can be coupled with the 2D fire spread model. This idea was first published  
24 in Asensio *et al.* (2002), where the coupling of wind and fire models had already been  
25 considered. The details of how this model stems from an asymptotic approximation of  
26 the Navier-Stokes equations can be found in Asensio *et al.* (2005). Roughly speaking,  
27 the HDWM locally provides a detailed 3D wind velocity field in an air layer over the  
28 surface, above which the surface temperature and topography have not effect, solving  
29 only 2D equations depending on the temperature on the ground surface  $T$  (or  $T_\infty$  in  
30 the absence of fire), topography  $h$ , and the horizontal component of the meteorological  
31 wind  $\mathbf{v}_m \cdot \mathbf{n}$  on the boundary of the simulation air layer. The model depends on a single  
32 parameter, the friction coefficient  $\zeta$ , which is related to the surface roughness length  $z_0$   
33 ( $m$ ) using the Davenport classification of terrain (Davenport *et al.* 2000). The model  
34 takes into account slope effects, mass conservation and buoyancy forces that enable the  
35 effect of wind temperature to be included. In Ferragut *et al.* (2011) the wind velocity field  
36 obtained by the model is adjusted to several wind velocity measurements  $\mathbf{v}_m$  at different  
37 points in the 3D domain. This adjustment requires solving an optimal control problem  
38 in which the wind flow on the surface boundary is the control. Our wind field model does  
39 not therefore require measuring the meteorological wind on the boundary, as it suffices  
40 to provide the meteorological wind at certain points in the domain, for example, the data  
41 from weather stations. Our model is an alternative for wind resource estimation in local  
42 terrains using mesoscale-microscale coupling techniques (Gopalan *et al.* 2014).

43 The HDWM equations are not shown in this paper due to their mathematical  
44 complexity. Interested readers can find the details in the above-mentioned papers. The  
45 implementation of the HDWM model is entered in the Spanish Registry of Intellectual  
46 Property on 16 July 2015 under record entry 00/2015/4721.

## 50 2.3. Coupling PhFFS-HDWM

51 Coupling both HDWM and PhFFS models reveals the influence that thermal effects,  
52 such as the high temperatures that occur during a fire, have on the wind, and the effect  
53 of wind (and also slope) on the flame tilt in order to compute the radiation and thus on  
54  
55  
56  
57  
58  
59  
60

1  
2  
3  
4 fire spread. The wind's effect on the fire model gauged through the convective term and  
5 the flame tilt in the radiation term is computed in a very competitive time. In general  
6 terms, the one-hour simulation of a medium size fire by the PhFFS model, updating wind  
7 data every half hour by the HDWM, is at least ten times faster than the actual period  
8 simulated. Considering that the fire's thermal effects on wind involves updating wind  
9 data each time step on fire simulation, significantly increasing final computational time.  
10 In order to reduce this time, improvements in the code parallelization are being studied,  
11 as well as the introduction of reduced basis methods for the HDWM model (Cascón *et al.*  
12 2016). We do not present coupled simulation results in this paper.  
13  
14  
15  
16  
17  
18  
19  
20

#### 21 2.4. Input variables, parameters and output variables

22 Since the aim of this work is to develop a tool that allows non-specialized users to simulate  
23 real fires in a user-friendly environment, it is important to identify the model input and  
24 output data, as a first step for integrating the PhFFS and HDWM models into the final  
25 GIS tool. Figure 1 summarizes the inputs and outputs of both models, as described in  
26 this section.  
27

28 Regarding the input data, we have distinguished between the input variables and the  
29 model parameters. The input variables are those magnitudes that can be measured more  
30 or less accurately, which together define a specific scenario for the modelling and the user  
31 should provide. Model parameters are unknown values, although their physical meaning  
32 can offer an approximate idea of their ranges, which should be previously adjusted. Tables  
33 1 and 2 summarise the parameters and the input variables (fuel type and no fuel type  
34 dependent) for PhFFS and HDWM, respectively.

35 The necessary meteorological data, ambient temperature  $T_{\infty}$  and wind velocity  $\mathbf{v}_m$ ,  
36 are provided by weather stations placed in or very close to the study areas. All the other  
37 input variables, such as the height of the surface  $h$  or the fuel load  $M$ , are spatial data,  
38 and must therefore be provided via GIS.

39 Among the spatial data needed for HDWM and PhFFS, it is important to mention fuel  
40 type, as most of the input variables depend on fuel type. It is currently considering the  
41 BEHAVE fuel classification system (Anderson 1982), but it may be used the more recent  
42 Scott and Burgan dynamic fuel models (Scott and Burgan 2005), or even monitored data  
43 whenever available. These data are obtained from land cover or forestry maps, and are  
44 used as an index to establish the model input variables dependent on them.

45 In addition, the PhFFS model needs two more spatial input variables related to the  
46 initial conditions in the study area. One is the initial solid fuel temperature,  $T$  at time  
47  $t = 0$ , which contains the information related to the ignition location. The other one is  
48 the initial fuel load,  $M$  at time  $t = 0$ , supplied by land cover maps that provide those  
49 points on the surface where combustibles spread the fire and those where there is no fuel,  
50 such as highways, rivers and lakes, etc.

51 We should recall that the corresponding non-dimensional initial solid fuel temperature  
52  $u = \frac{T - T_{\infty}}{T_{\infty}}$  and non-dimensional initial fuel load  $c = \frac{M}{M_0}$  are the unknowns of the PhFFS  
53 model. At each time step, the PhFFS model provides these two spatial output variables,  
54  $u$  and  $c$ , which will be displayed in the GIS tool.  
55  
56  
57  
58  
59  
60



### 3. Development of the GIS-based interface

This section describes all the details of the GIS interface development for the PhFFS and HDWM models, as outlined in Figure 2. This interface is implemented as a *Python add-in* for the ArcMap 10.4 application of Esri's ArcGIS Desktop suite<sup>1</sup>. We cover all the topics related to the automation of spatial data processing and user interface development. We then discuss the geographical resources used to provide the input data the models need, and finally, we also explain how the results obtained are displayed.

#### 3.1. User interface

The integration of GIS and spatio-temporal models has been widely studied, and many different approaches have been considered. These strategies can be categorized as follows (Goodchild *et al.* 1992, Nyerges 1992, Jankowski 1995, Malczewski 2006): *embedded coupling*, where there is full integration of the model within the GIS by creating user-specified routines with generic programming languages; *tight coupling*, where the model and the GIS are integrated under a common interface; and *loose coupling*, where the linkage between the GIS and the modelling system is made through the import-export of data.

The PhFFS and HDWM models have an interface provided through *ASCII grid text files* as inputs and outputs, so the easiest option for coupling these models with GIS software is a *loose coupling approach*, in which the GIS software is used to build these *ASCII grid text files* for each simulation scenario, calls the standalone executables of the models and reads their outputs in order to visualize them. This arrangement guarantees the same behaviour of the models both within or outside the GIS platform, reducing the amount of testing and validation required by the whole system. Adapting these models interface to GIS software involves redefining the input and output format files.

The GIS tool chosen for the integration of our models, ArcMap 10.4 of Esri's ArcGIS Desktop suite, provides options for expanding its features through custom tools. The interface with the PhFFS and HDWM models has been developed as a *Python add-in* for ArcMap. A *Python add-in* is a customization, such as a collection of tools on a toolbar, which plugs into an ArcGIS for Desktop application (ArcMap in this case) to provide supplemental functionality for performing customised tasks (ESRI 2016b).

The add-in developed includes a menu and a toolbar that contains a collection of custom tools designed to facilitate the use of the PhFFS and HDWM models. The functionality of each tool is implemented as a script using the Python programming language and the ArcPy geoprocessing library (ESRI 2016c). These scripts are run each time the user presses a button on the toolbar or on the menu, or fires a mouse event over the basemap.

Following the flow diagram in Figure 2, once we have loaded the basemap layer, we select the area of study and set the information over the basemap to simulate a specific scenario: ignition points, wind data, and eventually firebreaks, using the corresponding menu option or toolbar option or mouse event. All this information and the corresponding spatial data for the selected area are pre-processed: clipped, checked to avoid errors, converted to raster, and exported to ASCII grid text files. The PhFFS and HDWM read the files they need, and the simulation is run providing the corresponding output ASCII

<sup>1</sup>ArcGIS® and ArcMap™ are the intellectual property of Esri and are used herein under license. Copyright© Esri. All rights reserved. For more information about Esri® software, please visit [www.esri.com](http://www.esri.com).

1  
2  
3  
4 grid text files. The post-processing step converts the output ASCII files to raster and  
5 vector files in order to display them over the basemap. All the raster and vector layers  
6 used during the same simulation process are geo-referenced to the same geographical  
7 area, and have the same resolution and dimensions.

8 The integration of the PhFFS and HDWM models into a GIS tool achieves several  
9 objectives. First of all, it provides a simple, intuitive and easy-to-use tool that is more  
10 accessible to a broader audience that might not be familiar with PhFFS and HDWM  
11 models. Furthermore, the automation of the data acquisition and processing of all the  
12 geographical information required simplifies the simulation process reducing simulation  
13 time. It also prevents input data errors, which may cause software crashes or incorrect  
14 outputs, and ensures complete and reliable data, as well as the standardization of the geo-  
15 referenced input data. Therefore, the development of this operational system improves  
16 its usability by a reducing simulation time and user-knowledge.

### 17 18 19 20 **3.2. Input spatial data**

21 As we described in Section 2.4, our GIS-integrated wildland fire model uses the following  
22 input data: topography, fuel load and type, weather conditions, ignition location and  
23 fire suppression tactics; and predicts the fire spread for the established time period,  
24 providing the following outputs at each time step: the burnt area perimeter and the fire  
25 front position. Likewise, our GIS-integrated wind model also uses topography, surface  
26 roughness and weather conditions, and provides a wind velocity field that is well adapted  
27 to the domain studied, defined by wind velocity.

28 Initially, the GIS-based wildland fire simulation tool described in this paper was  
29 developed for its use throughout Spain, so the scope of the spatial information  
30 currently used is limited to that area. We define a common spatial reference for all  
31 the heterogeneous spatial data resources. According to Spanish regulations (BOE 2007),  
32 the selected spatial reference is the Projected Coordinate System *ETRS1989 UTM Zone*  
33 *30N*, except for the Canary Islands, where the Projected Coordinate System *ETRS1989*  
34 *UTM Zone 28N* is used instead. All the maps and databases we mention hereafter are  
35 referred to in English with their Spanish acronym, and the corresponding copyrights are  
36 shown in the references.

37 The first geographical resource is the basemap used to identify the area in which the  
38 simulation is to be conducted. The fire ignition point is located on the basemap by a  
39 simple mouse event, as well as possible fire suppression tactics and meteorological wind  
40 data positions. Finally, this map is also used to display the simulation results. Since  
41 basemaps are used in many applications, there are several options delivered as map  
42 services, ranging from public entities to private corporations, such as *ArcGIS online*  
43 *Basemaps* (ESRI 2016a). The basemap selected for our operating system is the *Spanish*  
44 *Topographic Basemap* provided by the © *Instituto Geográfico Nacional de España* (IGN)  
45 via a *Web Map Service* (WMS) (IGN 2016).

46 Once the study domain has been selected, we need three raster files corresponding  
47 to the topography, fuel type and fuel load of the study domain. In order to reduce  
48 computation time, we have gathered all the necessary resources as input data, and then  
49 we have processed them to produce a geodatabase that contains the three maps needed  
50 for extracting the spatial information our models use. In this way, for each simulation it  
51 is enough to clip the data corresponding to the study domain. It is important to stress  
52 that the scope for applying the system developed can be extended to other areas by  
53 incorporating the geographical information for a new region.

1  
2  
3  
4 The first map processed contains the height of the surface  $h$  required for both PhFFS  
5 and HDWM models. This information is provided by a *Digital Elevation Model* (DEM).  
6 We select the DEM also published by the IGN via a *Web Coverage Service* (WCS)  
7 (IGN 2013). The service offers DEMs with different resolutions -25, 200, 500 and 1,000  
8 metres- and different reference systems. The resolution selected is 25 metres, with the  
9 spatial reference mentioned above. Since one of the requirements of a fire spread model  
10 is to provide real-time feedback, as the WCS service response time penalizes the entire  
11 system response time, we extract the entire DEM for the whole of Spain, and store it on  
12 a geodatabase on the local hard drive.

13  
14 The second second map processed gathers all the information related to fuel type,  
15 provided by land cover or forestry maps. Depending on the region and/or year in which  
16 the fire to be simulated occurred, we use the *Spanish Forestry Map 1:25,000* (MFE25)  
17 (Magrama 2016b) combined with the *Fourth Spanish National Forest Inventory* (IFN4)  
18 (Magrama 2016a) or the *Spanish Forestry Map 1:50,000* (MFE50) (Magrama 2007a) with  
19 the information from the *Third Spanish National Forest Inventory* (IFN3) (Magrama  
20 2007b). Both inventories have been developed by the *Ministry of Agriculture, Food  
21 and Environment* of the Spanish Government. As explained in Section 2.4, fuel type  
22 is required as an index to set the fuel type dependent input variables for both PhFFS  
23 and HDWM models.

24 The third map processed collects all the elements involving the function of either  
25 artificial or natural fuelbreaks that affect the fire spread. These data have been extracted  
26 from the *Spanish Land Cover Information System* (SIOSE) (IGN 2011) by selecting  
27 all the surfaces where a fire can not occur (barren land, water bodies, transport  
28 infrastructures, etc.), providing zero load fuel data for the model. We should emphasise  
29 that the PhFFS model caters for fire crossing surfaces without fuel by the radiation  
30 mechanism. As mentioned above, the tool developed allows incorporating certain fire  
31 suppression tactics into the simulation process: the user can interactively insert firebreaks  
32 through a mouse event over the basemap, adding this new information to fuel load data.  
33 It is thus possible to overcome the limitations of the static nature of the GIS to adapt the  
34 simulation to the ongoing situation. From all these data, the initial fuel load is generated.

35  
36 Finally, the PhFFS model requires another last georeferenced data, the ignition points.  
37 These points are also introduced interactively over the basemap via mouse events. This  
38 information is passed to the model as the peak temperature of the solid fuel at the point  
39 where the mouse event took place, providing the initial solid fuel temperature.

40 Optional spatial data used by the PhFFS model involve wind velocity, which can either  
41 be computed by the HDWM model or a given value.

42 On the other hand, apart from the height  $h$  of the surface and the roughness length  
43  $z_0$ , the HDWM takes the surface air temperature at each point. Such data are provided  
44 as a raster that may reflect the fire's influence on local weather conditions.

### 45 46 47 **3.3. Mapping output data**

48 After processing the input data provided and running the models, the simulation results  
49 are displayed on the basemap. As mentioned at the end of Section 2.4, the PhFFS model  
50 provides two types of output data: the solid fuel mass fraction  $c$  and the non-dimensional  
51 solid fuel temperature  $u$ . Comparing the output solid fuel mass fraction with the initial  
52 fuel mass fraction inputted into the model provides the state of the landscape. So for  
53 each point of the domain we can determine whether or not that specific point has been  
54 burnt. This information is transformed to a vector layer and represented on the basemap  
55  
56  
57  
58  
59  
60

1  
2  
3  
4 in order to establish the *fire perimeter* at different instants, using a layer for each time  
5 step. The solid fuel temperature is also transformed into a vector layer and represented on  
6 the basemap for identifying those areas burning at the indicated time step, establishing  
7 the *fire front position* (see Figure 6 in the following section).

8 Likewise, the wind velocity data that the HDWM provides at different layers over the  
9 ground surface can be displayed. We represent the resulting wind field by combining  
10 this information on a feature class, and we use its attributes (module and direction) for  
11 setting the corresponding colors and arrows with the right rotation. As ArcMap can only  
12 visualize 2D scenarios, we represent the wind data corresponding to each level by using  
13 a different layer for each height level (see Figure 4).

#### 14 15 16 17 18 4. Example

19 The tool's functionality is tested by simulating a real fire that occurred in an area near  
20 Ourense (Spain) in August, 2009, comparing the simulation results with the actual fire  
21 data. The results from the simulations of this scenario indicate acceptable agreement,  
22 showing that the combination of the PhFFS model with GIS can simulate realistic  
23 wildland fire scenarios, in faster than real-time. The simulation area is a rectangle of  
24  $3.315\text{ m} \times 2.740\text{ m}$ , and the simulation of each hour of fire spread involves about 4.30  
25 minutes of computational time on a laptop equipped with an Intel i5-2410M processor  
26 (two cores, each one working at a frequency of 2.30 GHz) and 8 GB RAM. A total of  
27 4 hours and a half have been simulated, reporting results every 15 minutes of real-time  
28 simulation and updating wind data every half hour, with a total simulation time of 20  
29 minutes.

30  
31 The real wildfire ignited at 3.45 p.m. local time on 17 August 2009 near Osoño, Ourense  
32 province, in the autonomous region of Galicia in north-western Spain, one of the country's  
33 most fire-affected areas. The fire-fighting team had failed to stabilise the fire by 11.00  
34 p.m. on the same day, but brought it under control at 3.45 a.m. on the following day, and  
35 finally extinguishing it at 9.10 p.m. on 18 August. The fire burned 224 ha: 185 ha of forest  
36 area (83 ha. were tree-covered interspersed with heath) and 39 ha. of agricultural area.  
37 The fire spread and its behaviour were reconstructed and documented by the coordinator  
38 of the fire-suppression operations, A. Morillo (2011), co-author of this paper.

39 The burnt area is located at an altitude ranging from 540 metres (ignition point area)  
40 to 680 metres (end fire area) above sea level. The average slope ranges from 6.56% at  
41 the beginning of the fire, to 2.86% at the end. For the first hours, the fire spread over  
42 an uneven surface, with positive and negative discontinuous slopes, with watersheds and  
43 river basins; for the final part, although the altitude is higher, the surface is relatively  
44 flat.

45 Figure 3 shows the fuel data from the IFN4 with the fuel type distribution according  
46 to BEHAVE classification (Andrews 1986), adapted to Spanish forestry by the Nature  
47 Conservation Institute (MAPA 1987). The IFN4 data show some discrepancies with the  
48 observed data because the area where this fire occurred has been affected by several fires  
49 over the years, and these data are not regularly updated. This discrepancy between the  
50 available data and the actual data poses one of the challenges that fire simulation has  
51 to tackle. In this example, the initial burnt area was covered mainly with *Pinus pinaster*  
52 corresponding to model 7 (inflammable brush); the middle area was covered with model  
53 6 (dormant brush) and to a lesser extent model 1 (short grass) and 2 (timber grass). The  
54 end burnt area was covered with diverse fuel types, mainly model 5 (brush). Basin areas  
55  
56  
57  
58  
59  
60

1  
2  
3  
4 and property lines were covered by thick forest, corresponding to model 9 (dense forest)  
5 but these data do not appear in the IFN4 database. The observed data show areas with  
6 some shrubs in the middle and end areas that do not appear in the IFN4 data. Figure  
7 3 also shows the existing fuelbreaks (20 m wide) along the crests that the actual fire  
8 crossed, as did the simulation, and two firebreaks (red lines) the fire-fighters made by  
9 widening two existing roads on the southern flank.

10 Table 3 summarizes the values of the fuel type dependent input variables used in the  
11 example for each one of the five fuel types that appear in the IFN4 data on the studied  
12 area. These values have been identified adapting the information from Arellano *et al.*  
13 (2016) to the BEHAVE classification for the PhFFS model fuel type dependent input  
14 variables. The values for the roughness length  $z_0$  used for the HDWM are taken from  
15 Wieringa (1992).

16 Weather data (wind, temperature and relative humidity) were collected every ten  
17 minutes at a nearby weather station (3750 m away) at a height of 10 m and were  
18 incorporated into the simulation process every 30 minutes. Table 4 summarizes the  
19 average hourly ambient temperature (Celsius), relative air humidity (%), wind speed  
20 (m/s) and direction (degree from North), and wind gust (m/s). Figure 4 shows the wind  
21 field simulated with the HDWM at a height of 10 meters, corresponding to meteorological  
22 data at 7.00 p.m.

23 The coupling effect of wind and topography considerably influenced this fire spread rate  
24 and direction. Initially, wind velocity was moderate, about  $3.18\text{ m/s}$  from the west. As the  
25 afternoon progressed the wind velocity increased to  $4.79\text{ m/s}$  with gusts of almost  $8\text{ m/s}$ ,  
26 and turning slightly to the north. This caused secondary fire sources due to the transport  
27 of firebrands by convection columns. Most of the fire-fighters' actions by land and air over  
28 the fire flanks are not reflected in the simulation, nor are the secondary fire sources, due  
29 to insufficient information, except those firebreaks made by widening some existing roads,  
30 where the available information is sufficiently detailed. Despite that, the simulated and  
31 actual perimeters are quite similar, as shown in Figure 5, where the actual and simulated  
32 perimeters at 5.00 p.m., 6.00 p.m., 7.00 p.m. and 8.00 p.m. are outlined together with  
33 the corresponding Sørensen similarity index ( $S$ ), Jaccard similarity coefficient ( $J$ ) and  
34 Kappa coefficient ( $K$ ) (Filippi *et al.* 2014). These coefficients range from 0 and 1; 1  
35 means a perfect agreement between observation and simulation, and 0 means there is  
36 no agreement. The average values obtained,  $\bar{S} = 0.74$ ,  $\bar{J} = 0.59$  and  $\bar{K} = 0.71$ , show  
37 *substantial agreement* (Filippi *et al.* 2014). The largest differences between the actual  
38 and simulated perimeters arises in the latest instant due to the increased fire-fighters'  
39 actions not reflected in the simulation (see Figure 5(d)).

40 Figure 6 shows the actual perimeter (black line) and simulated fire at 7.00 p.m. in  
41 the GIS interface. The simulated fire differentiates between active fire front (orange) and  
42 burnt area (grey).

## 43 5. Conclusions

44 This paper presents a GIS-based interface for two simplified physical models, a wildland  
45 fire spread model, PhFFS, and a wind field model, HDWM, which can work coupled  
46 or separately. The development of this tool is based on the extent of the functionality  
47 of the GIS commercial software ArcGIS, through the Python scripting language and  
48 Esri's ArcPy library. Several scripts have been developed to automate geographical  
49 data acquisition, spatial data pre-processing, model running, and the visualization of  
50  
51  
52  
53  
54  
55  
56  
57  
58  
59  
60



1  
2  
3  
4 the simulation results on a basemap.

5 The initial purpose of the integration of the fire and wind models on a GIS-based  
6 interface is to facilitate the testing and validation process, by automating and simplifying  
7 the data acquisition process and the display of the solution.

8 The GIS-based tool achieves a second purpose, as it makes the PhFFS and HDWM  
9 models more readily accessible to the potential end-user by providing a simple, intuitive  
10 and easy-to-use tool that is more accessible to a broader audience that might not be  
11 familiar with these models.

12 The complete simulation of either one of the physical processes that the tool supports,  
13 wildland fire spread or wind field, includes three steps: pre-processing the requested  
14 data, calculating the models, and post-processing the solution. The scripts developed  
15 reduce pre-processing and post-processing times and prevent input data errors. The  
16 numerical techniques that both PhFFS and HDWM use guarantee shorter-than-real-time  
17 computational times. Reducing the total computational time is critical for the practical  
18 application of these models.

19 Some direct applications of the PhFFS model are the design of risk mapping,  
20 reforestation policies, or fuelbreaks in prevention operations; the optimization of fire-  
21 fighting resources, risk prevention, the issue of warnings or evacuation planning in  
22 suppression operations, along with others such as prescribed burn planning.

23 Certain additional functionalities of the designed tool may have an interesting potential  
24 for practical applications. Secondary fire sources (spotting) can be simulated by adding  
25 new ignition points. Some suppression works, such as firebreaks, can be simulated through  
26 the "firebreaks tool" on the application toolbar, enabling the user to test different  
27 scenarios.

28 The HDWM has other specific applications, such as wind power forecasting on wind  
29 farms.

30 Finally, the real analysed wildland fire pointed out the utility of the system through  
31 a realistic simulation of the wildfire spread, showing a substantial agreement between  
32 simulation and observation.

### 33 34 35 36 37 38 **Acknowledgments**

39 This work has been partially supported by the Department of Education of the regional  
40 government, *Junta of Castilla y León*, Grant contract: SA020U16 with the participation  
41 of FEDER, and by *University of Salamanca General Foundation*, TCUE grant. The  
42 authors are also grateful to Blanca Ruiz Franco, head of the Nature Databank of the  
43 Ministry of Agriculture, Food and the Environment of the Spanish Government for her  
44 technical support, providing the Spanish Forestry Map 1:25.000.

### 45 46 47 48 49 **Notes**

50 Maps throughout this paper were created using ArcGIS<sup>®</sup> software by Esri. ArcGIS<sup>®</sup> and  
51 ArcMap<sup>™</sup> are the intellectual property of Esri and are used herein under license.  
52 Copyright<sup>©</sup> Esri. All rights reserved. For more information about Esri<sup>®</sup> software, please  
53 visit [www.esri.com](http://www.esri.com).

## References

- 1  
2  
3  
4  
5  
6  
7  
8  
9  
10  
11  
12  
13  
14  
15  
16  
17  
18  
19  
20  
21  
22  
23  
24  
25  
26  
27  
28  
29  
30  
31  
32  
33  
34  
35  
36  
37  
38  
39  
40  
41  
42  
43  
44  
45  
46  
47  
48  
49  
50  
51  
52  
53  
54  
55  
56  
57  
58  
59  
60
- Ager, A.A., Vaillant, N.M., and Finney, M.A., 2011. Integrating Fire Behavior Models and Geospatial Analysis for Wildland Fire Risk Assessment and Fuel Management Planning. *Journal of Combustion*, 2011, 1–19.
- Anderson, H.E., 1969. *Heat transfer and Forest Fire*. General Technical Report INT-69, U.S. Department of Agriculture, Forest Service, Intermountain Forest and Range Experiment Station, Ogden, UT.
- Anderson, H., 1982. *Aids to Determining Fuel Models for Estimating Fire Behavior*. General Technical Report INT-122, U.S. Department of Agriculture, Forest Service, Intermountain Forest and Range Experiment Station.
- Andrews, P., 1986. *Behave: fire behaviour prediction and fuel modellings system - burn subsystem, part 1*. General Technical Report INT-194, U.S. Department of Agriculture, Forest Service, Intermountain Forest and Range Experiment Station, Ogden, UT.
- Arellano, S., et al., 2016. *Foto-Guía de combustibles forestales de Galicia*. Santiago de Compostela: Andavira Editora, S.L.
- Asensio, M. and Ferragut, L., 2002. On a wildland fire model with radiation. *International Journal for Numerical Methods in Engineering*, 54 (1), 137–157.
- Asensio, M., Ferragut, L., and Simon, J., 2002. Modelling of convective phenomena in forest fire. *RACSAM - Revista de la Real Academia de Ciencias Exactas, Físicas y Naturales. Serie A. Matemáticas*, 96 (3), 299–313.
- Asensio, M., Ferragut, L., and Simon, J., 2005. A convection model for fire spread simulation. *Applied Mathematics Letters*, 18 (6), 673–677 Special issue on the occasion of MEGA 2003.
- BOE, 2007. Real Decreto 1071/2007, de 27 de julio, por el que se regula el sistema geodésico de referencia oficial en España.. *Boletín Oficial del Estado* [online] Available from: [http://www.fomento.gob.es/NR/rdonlyres/5B614FA3-5B57-4838-9D08-1434B8FD2DD5/70540/RD\\_1071\\_2007.pdf](http://www.fomento.gob.es/NR/rdonlyres/5B614FA3-5B57-4838-9D08-1434B8FD2DD5/70540/RD_1071_2007.pdf), [in Spanish] [Retrieved: May, 2016].
- Cascón, J., et al., 2016. A reduced basis for a local high definition wind model. *Computer Methods in Applied Mechanics and Engineering*, 311, 438 – 456.
- Chapman, B., Jost, G., and Pas, R.V.D., 2008. *Using OpenMP: Portable Shared Memory Parallel Programming*. Scientific and Engineering Computation MIT Press.
- Chuvieco, E. and Duarte, L., 1996. Mapping the spatial distribution of forest fire danger using GIS. *International Journal of Geographical Information Science*, 10 (3), 333–345.
- Coleman, J. and Sullivan, A., 1996. A real-time computer application for the prediction of fire spread across the Australian landscape. *Simulation*, 67, 230–240.
- Davenport, A., et al., 2000. Estimating the roughness of cities and sheltered country. *In: Preprints Twelfth Conference on Applied Climatology*, Asheville, N.C., United States American Meteorological Society, 96–99.
- ESRI, 2016a. ArcGIS Online Basemaps. [online] Available from: <http://www.esri.com/data/basemaps> [Retrieved: May, 2016a].
- ESRI, 2016b. What is a Python add-in?. *Help documents collection from ArcGIS Online* [online] Available from: <http://desktop.arcgis.com/en/arcmap/10.3/guide-books/python-addins/what-is-a-python-add-in.htm> [Retrieved: May, 2016b].
- ESRI, 2016c. What is ArcPy?. *Help documents collection from ArcGIS Online* [online] Available from: <https://desktop.arcgis.com/en/arcmap/10.3/analyze/arcpy/what-is-arcpy-.htm> [Retrieved: May, 2016c].

- 1  
2  
3  
4  
5  
6  
7  
8  
9  
10  
11  
12  
13  
14  
15  
16  
17  
18  
19  
20  
21  
22  
23  
24  
25  
26  
27  
28  
29  
30  
31  
32  
33  
34  
35  
36  
37  
38  
39  
40  
41  
42  
43  
44  
45  
46  
47  
48  
49  
50  
51  
52  
53  
54  
55  
56  
57  
58  
59  
60
- FAO, 2007. *Fire-management global assessment 2006. A thematic study in the framework of the Global Forest Resources Assessment 2005.*. Technical report FAO Forestry Paper 151, Food and Agriculture Organization of the United Nations, Rome.
- Ferragut, L., *et al.*, 2014. No. 4 SEMA SIMAI Springer Series, A Simplified Wildland Fire Model Applied to a Real Case. *In: Advances in Differential Equations and Applications.*, 155–167 Cham: Springer International Publishing.
- Ferragut, L., *et al.*, 2015. A Wildland Fire Physical Model Well Suited to Data Assimilation. *Pure and Applied Geophysics*, 172 (1), 121–139.
- Ferragut, L., Asensio, M., and Monedero, S., 2007a. Modelling radiation and moisture content in fire spread. *Communications in Numerical Methods in Engineering*, 23 (9), 819–833.
- Ferragut, L., Asensio, M., and Monedero, S., 2007b. A numerical method for solving convection-reaction-diffusion multivalued equations in fire spread modelling. *Advances in Engineering Software*, 38 (6), 366–371.
- Ferragut, L., Asensio, M., and Simon, J., 2011. High definition local adjustment model of 3D wind fields performing only 2D computations. *International Journal for Numerical Methods in Biomedical Engineering*, 27 (4), 510–523.
- Filippi, J., Mallet, V., and Nader, B., 2014. Representation and evaluation of wildfire propagation simulations. *International Journal of Wildland Fire*, 23, 46–57.
- Finney, M., 2004. *FARSITE: Fire Area Simulator model development and evaluation.*. Research Paper RMRS-RP-4 (revised), U.S. Department of Agriculture, Forest Service, Rocky Mountain Research Station, Ogden, UT.
- Finney, M., *et al.*, 2015. Role of buoyant flame dynamics in wildfire spread. *Proceedings of the National Academy of Sciences of the United States of America*, 112 (32), 9833–9838.
- Flannigan, M.D., *et al.*, 2009. Implications of changing climate for global wildland fire. *International Journal of Wildland Fire*, 18 (5), 483–507.
- Frankman, D., *et al.*, 2013. Measurements of convective and radiative heating in wildland fires. *International Journal of Wildland Fire*, 22 (2), 157–167.
- Goodchild, M., *et al.*, 1992. Integrating GIS and spatial data analysis: problems and possibilities. *International Journal of Geographical Information Systems*, 6 (5), 407–423.
- Gopalan, H., *et al.*, 2014. A coupled mesoscale-microscale framework for wind resource estimation and farm aerodynamics. *Journal of Wind Engineering and Industrial Aerodynamics*, 132, 13 – 26.
- Hilton, J., *et al.*, 2015. Effects of spatial and temporal variation in environmental conditions on simulation of wildfire spread. *Environmental Modelling & Software*, 67, 118 – 127.
- IGN, 2011. Spanish Land Cover Information System. *Instituto Geográfico Nacional de España* [online] Available from: <http://www.ign.es/ign/layoutIn/siose.do> [Retrieved: May, 2016].
- IGN, 2013. Spanish Digital Elevation Model. *Instituto Geográfico Nacional de España* [online] Available via a Web Coverage Service from: <http://www.ign.es/wcs/mdt> [Retrieved: May, 2016].
- IGN, 2016. IGN Spanish Base Map. *Instituto Geográfico Nacional de España* [online] Available via a Web Map Service from: <http://www.ign.es/wms-inspire/ign-base> [Retrieved: May, 2016].
- Jankowski, P., 1995. Integrating geographical information systems and multiple criteria decision-making methods. *International Journal of Geographical Information Sys-*

- 1  
2  
3  
4  
5  
6  
7  
8  
9  
10  
11  
12  
13  
14  
15  
16  
17  
18  
19  
20  
21  
22  
23  
24  
25  
26  
27  
28  
29  
30  
31  
32  
33  
34  
35  
36  
37  
38  
39  
40  
41  
42  
43  
44  
45  
46  
47  
48  
49  
50  
51  
52  
53  
54  
55  
56  
57  
58  
59  
60
- tems, 9 (3), 251–273.
- Linn, R., et al., 2002. Studying wildfire behavior using FIRETEC. *International Journal of Wildland Fire*, 11 (4), 233–246.
- Linn, R.R., 1997. *A transport model for prediction of wildfire behavior*. Technical report LA-13334T, Los Alamos National Lab., NM (United States).
- Lopes, A., Cruz, M., and Viegas, D., 2002. FireStation - an integrated software system for the numerical simulation of fire spread on complex topography. *Environmental Modelling & Software*, 17 (3), 269 – 285.
- Magrama, 2007a. Spanish Forestry Map 1:50,000. *Ministerio de Agricultura, Alimentación y Medio Ambiente* [online], 3 (4). Available from: <http://www.magrama.gob.es/es/biodiversidad/servicios/banco-datos-naturaleza/informacion-disponible/mfe50.aspx> [Retrieved: May 2016a].
- Magrama, 2007b. Third Spanish National Forest Inventory. *Ministerio de Agricultura, Alimentación y Medio Ambiente* [online] Available from: <http://www.magrama.gob.es/es/biodiversidad/servicios/banco-datos-naturaleza/informacion-disponible/ifn3.aspx> [Retrieved: May 2016b].
- Magrama, 2016a. Fourth Spanish National Forest Inventory. *Ministerio de Agricultura, Alimentación y Medio Ambiente* [online] Available from: <http://www.magrama.gob.es/es/desarrollo-rural/temas/politica-forestal/inventario-cartografia/inventario-forestal-nacional/> [Retrieved: May 2016a].
- Magrama, 2016b. Spanish Forestry Map 1:25,000. *Ministerio de Agricultura, Alimentación y Medio Ambiente* [online] Available from: [http://www.magrama.gob.es/es/desarrollo-rural/temas/politica-forestal/inventario-cartografia/mapa-forestal-espana/mfe\\_25.aspx](http://www.magrama.gob.es/es/desarrollo-rural/temas/politica-forestal/inventario-cartografia/mapa-forestal-espana/mfe_25.aspx) [Retrieved: May 2016b].
- Malczewski, J., 2006. GIS-based multicriteria decision analysis: a survey of the literature. *International Journal of Geographical Information Science*, 20 (7), 703–726.
- Mandel, J., et al., 2014. Recent advances and applications of WRF-SFIRE. *Natural Hazards and Earth System Sciences*, 14, 2829–2845.
- Mandel, J., Beezley, J.D., and Kochanski, A.K., 2011. Coupled atmosphere-wildland fire modeling with WRF 3.3 and SFIRE 2011. *Geoscientific Model Development*, 4 (3), 591–610.
- MAPA, 1987. *Photographic key to the identification of fuel models*. Technical report, Ministerio de Agricultura Pesca y Alimentación, Instituto para la Conservación de la Naturaleza ICONA, Madrid [in Spanish].
- Morillo, A., 2011. *Análisis del comportamiento del fuego forestal observado y simulado: Estudio del caso del incendio forestal de Osoño (Vilardevós)-Verín-Ourense*. Master of advances studies work, Higher Politechnical School of Lugo, University of Santiago de Compostela, Spain (in Spanish).
- Nyerges, T., 1992. Coupling GIS and Spatial Analytical Models. In: P. Bresnahan, E. Corwin and D. Cowen, eds. *Proceedings of fifth International Symposium on Spatial Data Handling*, Asheville, N.C., United States Charleston, SC.: Humanities and Social Sciences Computing Laboratory, University of South Carolina, 534–543.
- Pastor, E., et al., 2003. Mathematical models and calculation systems for the study of wildland fire behaviour. *Progress in Energy and Combustion Science*, 29 (2), 139–153.
- Perry, G., Sparrow, A., and Owens, I., 1999. A GIS-supported model for the simulation of the spatial structure of wildland fire, Cass Basin, New Zealand. *Journal of Applied*

- 1  
2  
3  
4  
5  
6  
7  
8  
9  
10  
11  
12  
13  
14  
15  
16  
17  
18  
19  
20  
21  
22  
23  
24  
25  
26  
27  
28  
29  
30  
31  
32  
33  
34  
35  
36  
37  
38  
39  
40  
41  
42  
43  
44  
45  
46  
47  
48  
49  
50  
51  
52  
53  
54  
55  
56  
57  
58  
59  
60
- Ecology*, 36 (4), 502–518.
- Prieto, D., *et al.*, 2015. Sensitivity analysis and parameter adjustment in a simplified physical wildland fire model. *Advances in Engineering Software*, 90, 98–106.
- Reisner, J., Bossert, J., and Winterkamp, J., 1997. *Numerical Simulations of Two Wild-fire Events Using a Combined Modeling System (HIGRAD/ BEHAVE)*. Technical report LA-UR-97-4036, Los Alamos National Lab., NM (USA).
- Rothermel, P., 1972. *A mathematical model for predicting fire spread in wildland fuels*. Research Paper INT-115, U.S. Department of Agriculture, Forest Service.
- Scott, J. and Burgan, R., 2005. *Standard Fire Behavior Fuel Models: A Comprehensive Set for Use with Rothermel's Surface Fire Spread Model*. General Technical Report RMRS-GTR-153, U.S. Department of Agriculture, Forest Service, Rocky Mountain Research Station.
- Skidmore, A., 2002. *Environmental Modelling with GIS and Remote Sensing*. London: Taylor & Francis.
- Sullivan, A., 2009a. Wildland surface fire spread modelling, 1990-2007. 1: Physical and quasi-physical models. *International Journal of Wildland Fire*, 18 (4), 349–368.
- Sullivan, A., 2009b. Wildland surface fire spread modelling, 1990-2007. 2: Empirical and quasi-empirical models. *International Journal of Wildland Fire*, 18 (4), 369–386.
- Tymstra, C., *et al.*, 2010. *Development and structure of Prometheus: the Canadian wild-land fire growth simulation model*. Information Report NOR-X-417, Canadian Forest Service, Northern Forestry Centre.
- Vasconcelos, M. and Guertin, D., 1992. FIREMAP - Simulation of Fire Growth with a Geographic Information System. *International Journal of Wildland Fire*, 2 (2), 87–96.
- Viegas, D., 2004. Slope and wind effects on fire propagation. *International Journal of Wildland Fire*, 13 (2), 143–156.
- Wieringa, J., 1992. Updating the Davenport roughness classification. *Journal of Wind Engineering and Industrial Aerodynamics*, 41 (1), 357 – 368.
- Williams, T.M., Williams, B.J., and Song, B., 2014. Modeling a historic forest fire using GIS and FARSITE. *Mathematical & Computational Forestry & Natural Resource Sciences*, 6 (2).
- Yassemi, S., Dragievi, S., and Schmidt, M., 2008. Design and implementation of an integrated GIS-based cellular automata model to characterize forest fire behaviour. *Ecological Modelling*, 210 (12), 71–84.



## Tables

Table 1. PhFFS quantities, input variables and parameters.

Model quantities	Symbol	Units
Enthalpy	$E$	$J m^{-2}$
Solid fuel temperature	$T$	$K$
Fuel load	$M$	$kg m^{-2}$
Model input variables	Symbol	Units
<i>No fuel type dependent</i>		
Wind velocity	$\mathbf{V}$	$m s^{-1}$
Reference temperature	$T_{\infty}$	$K$
Surface height	$h$	$m$
Latent evaporation heat	$\Lambda_v$	$J kg^{-1}$
<i>Fuel type dependent</i>		
Maximum fuel load	$M_0$	$kg m^{-2}$
Moisture content	$M_v$	$kg$ of water/ $kg$ of dry fuel
Flame temperature	$T_f$	$K$
Pyrolysis temperature	$T_p$	$K$
Combustion half-life	$t_{1/2}$	$s$
Flame length	$F$	$m$
Heat capacity	$C$	$J K^{-1} kg^{-1}$
Model parameters	Symbol	Units
Mean absorption coefficient	$a$	$m^{-1}$
Natural convection coefficient	$H$	$J s^{-1} m^{-2} K^{-1}$
Correction factor of convective term	$\beta$	–

Table 2. HDWM quantities, input variables and parameters.

Model quantities	Symbol	Units
Wind velocity	$\mathbf{V}$	$m s^{-1}$
Potential	$p$	$s^{-1}$
Model input variables	Symbol	Units
<i>No fuel type dependent</i>		
Horizontal component of meteorological wind	$\mathbf{v}_m$	$m s^{-1}$
Surface air temperature	$T$	$K$
Height of the surface	$h$	$m$
<i>Fuel type dependent</i>		
Roughness length	$z_0$	$m$
Model parameters	Symbol	Units
Friction coefficient	$\zeta$	–

Table 3. Used values for fuel type dependent input variables.

Fuel type	Description	$M_0 (kgm^{-2})$	$M_v$	$T_f (K)$	$T_p (K)$	$t_{1/2} (s)$	$F (m)$	$C (JK^{-1}kg^{-1})$	$z_0 (m)$
1	Short grass	0.1	0%	1300	500	100	2.5	1800	0.08
2	Timber grass	1.0	10%	1300	500	100	4	2000	0.08
5	Brush	2.3	10%	1300	500	200	5.5	2300	0.1
6	Dormant brush	2.2	10%	1300	500	200	7	2300	0.1
7	Inflammable brush	2.4	15%	1300	500	200	8	2300	0.1

Table 4. Meteorological data.

Local time	Temperature ( $^{\circ}C$ )	Humidity (%)	Wind speed ( $m/s$ )	Wind direction	Wind gust ( $m/s$ )
3.45-5.00 p.m. average	32.02	27.17	3.18	319.39	5.62
5.00-6.00 p.m. average	32.01	27.43	4.79	341.29	7.76
6.00-7.00 p.m. average	31.50	27.43	4.42	334.00	7.44
7.00-8.00 p.m. average	31.42	27.50	4.48	335.00	7.45
8.00-9.00 p.m. average	30.11	30.00	4.42	344.33	7.24

## Figure Captions

Figure 1.. PhFFS and HDWM input and output data.

Figure 2.. GIS-PhFFS-HDWM integration flow diagram.

Figure 3.. Simulation area (red rectangle), fire ignition point, IFN4 fuel type distribution, actual final perimeter (black line) and fire-fighters' firebreaks (red lines).

Figure 4.. Screenshot of the GIS interface displaying the wind field simulated with HDWM at 7.00 p.m., at a height of 10 m, along the simulation area.

Figure 5.. Comparison of the actual (grey) and simulated (orange) perimeter at 5.00 p.m. (a), 6.00 p.m. (b), 7.00 p.m. (c) and 8.00 p.m. (d), and the corresponding Sørensen similarity index ( $S$ ), Jaccard similarity coefficient ( $J$ ), and Kappa coefficient ( $K$ ).

Figure 6.. Screenshot of the GIS interface displaying the actual perimeter (black line) and simulated fire: burnt area (grey) and active fire front (orange) after 3.15 hours of fire ignition (7.00 p.m.).

1  
2  
3  
4 **Figures**  
5

6 Figure 1. PhFFS and HDWM input and output data.  
7  
8  
9  
10

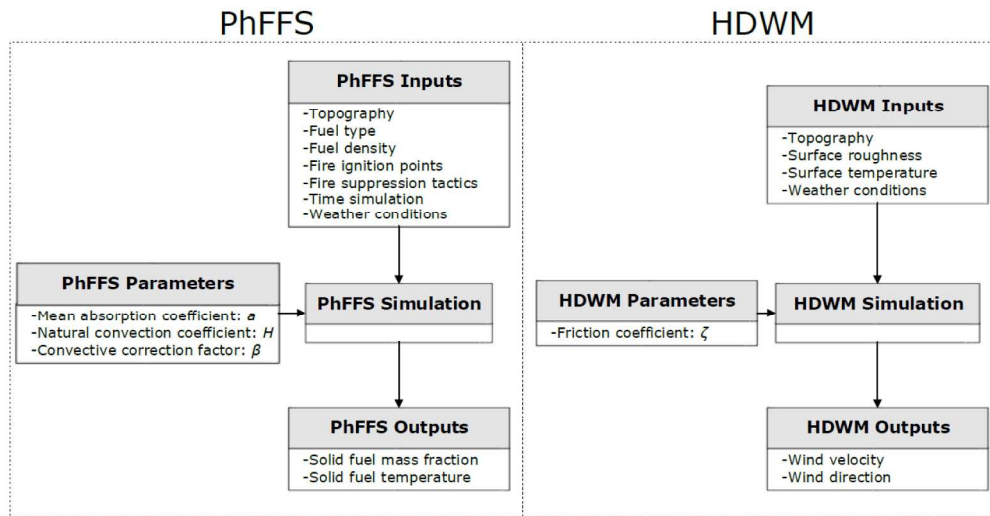
11  
12  
13  
14  
15  
16  
17  
18  
19  
20  
21 Figure 2. GIS-PhFFS-HDWM integration flow diagram.  
22  
23  
24  
25  
26  
27  
28  
29  
30  
31  
32  
33  
34

35 Figure 3. Simulation area (red rectangle), fire ignition point, IFN4 fuel type distribution, actual  
36 final perimeter (black line) and fire-fighters' firebreaks (red lines).  
37

38  
39 Figure 4. Screenshot of the GIS interface displaying the wind field simulated with HDWM at  
40 7.00 p.m., at a height of 10 m, along the simulation area.  
41

42 Figure 5. Comparison of the actual (grey) and simulated (orange) perimeter at 5.00 p.m. (a),  
43 6.00 p.m. (b), 7.00 p.m. (c) and 8.00 p.m. (d), and the corresponding Sørensen similarity index  
44 ( $S$ ), Jaccard similarity coefficient ( $J$ ), and Kappa coefficient ( $K$ ).  
45  
46

47 Figure 6. Screenshot of the GIS interface displaying the actual perimeter (black line) and sim-  
48 ulated fire: burnt area (grey) and active fire front (orange) after 3.15 hours of fire ignition (7.00  
49 p.m.).  
50  
51  
52  
53  
54  
55  
56  
57  
58  
59  
60

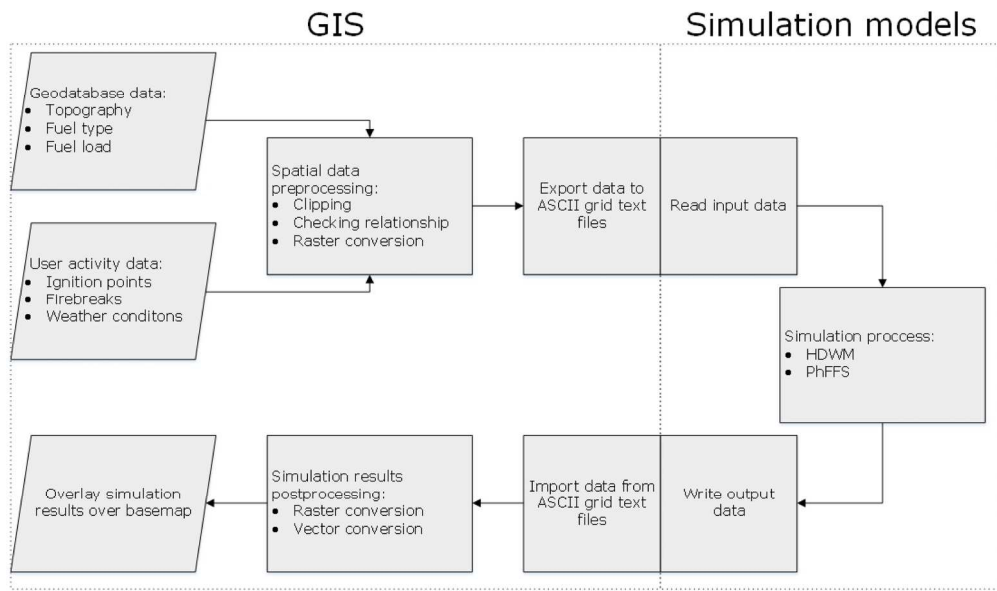


PhFFS and HDWM input and output data.

231x118mm (300 x 300 DPI)



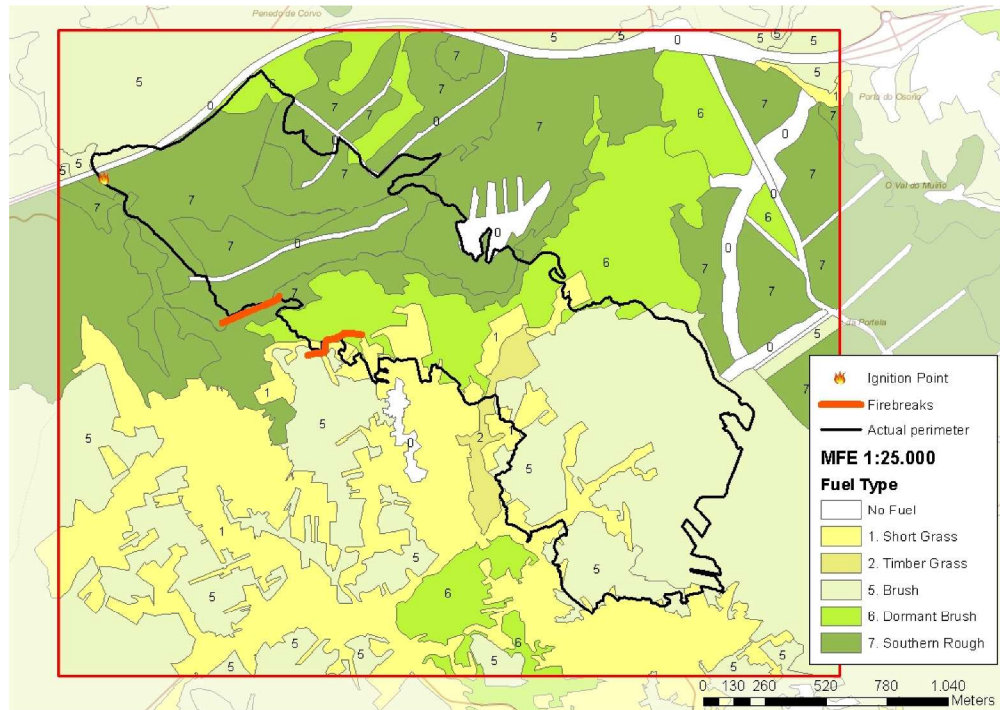
1  
2  
3  
4  
5  
6  
7  
8  
9  
10  
11  
12  
13  
14  
15  
16  
17  
18  
19  
20  
21  
22  
23  
24  
25  
26  
27  
28  
29  
30  
31  
32  
33  
34  
35  
36  
37  
38  
39  
40  
41  
42  
43  
44  
45  
46  
47  
48  
49  
50  
51  
52  
53  
54  
55  
56  
57  
58  
59  
60



GIS-PhFFS-HDWM integration flow diagram.

176x105mm (300 x 300 DPI)

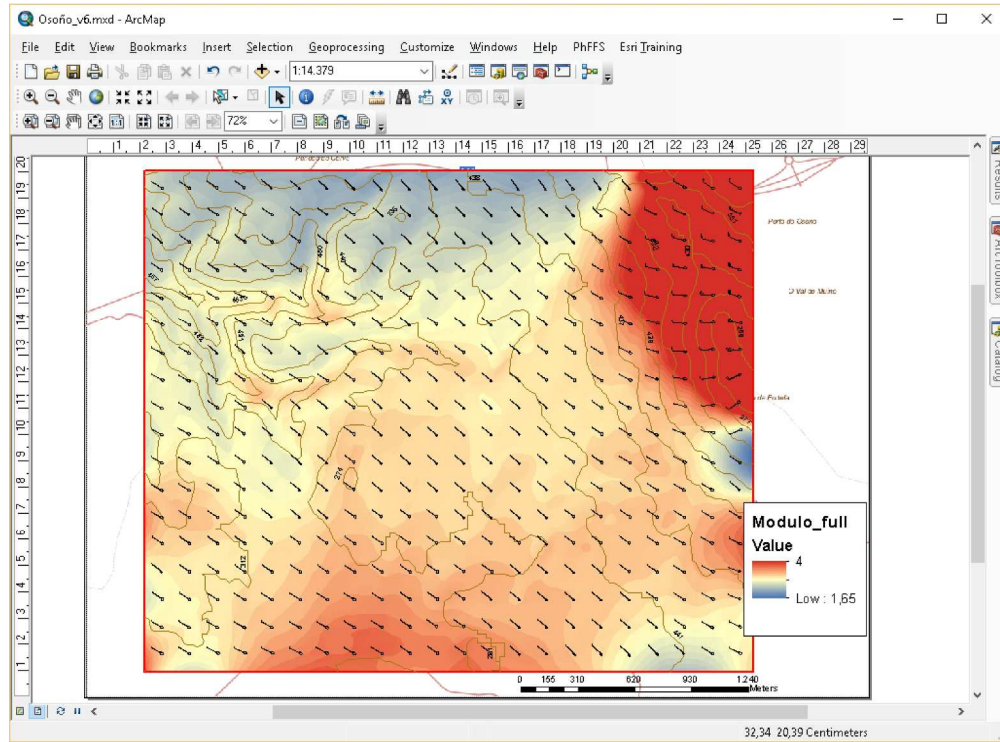
Review Only



Simulation area (red rectangle), fire ignition point, IFN4 fuel type distribution, actual final perimeter (black line) and fire-fighters' firebreaks (red lines).

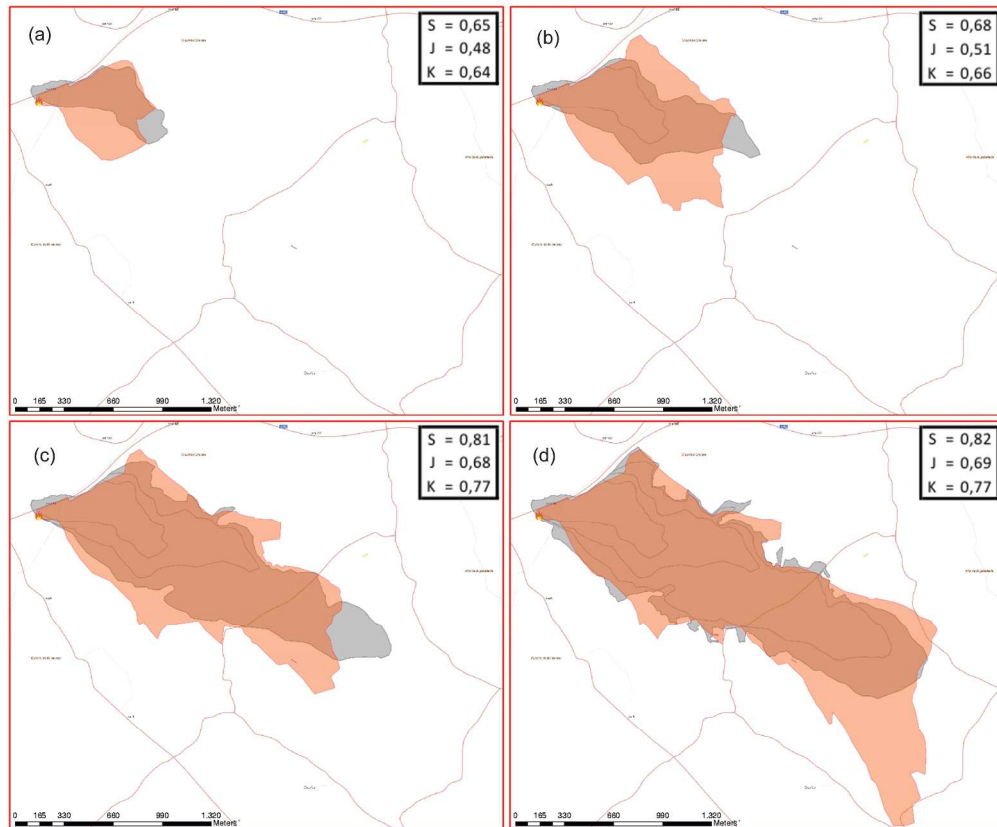
594x420mm (600 x 600 DPI)

1  
2  
3  
4  
5  
6  
7  
8  
9  
10  
11  
12  
13  
14  
15  
16  
17  
18  
19  
20  
21  
22  
23  
24  
25  
26  
27  
28  
29  
30  
31  
32  
33  
34  
35  
36  
37  
38  
39  
40  
41  
42  
43  
44  
45  
46  
47  
48  
49  
50  
51  
52  
53  
54  
55  
56  
57  
58  
59  
60



Screenshot of the GIS interface displaying the wind field simulated with HDWM at 7.00 p.m., at a height of 10 m, along the simulation area.

268x198mm (300 x 300 DPI)

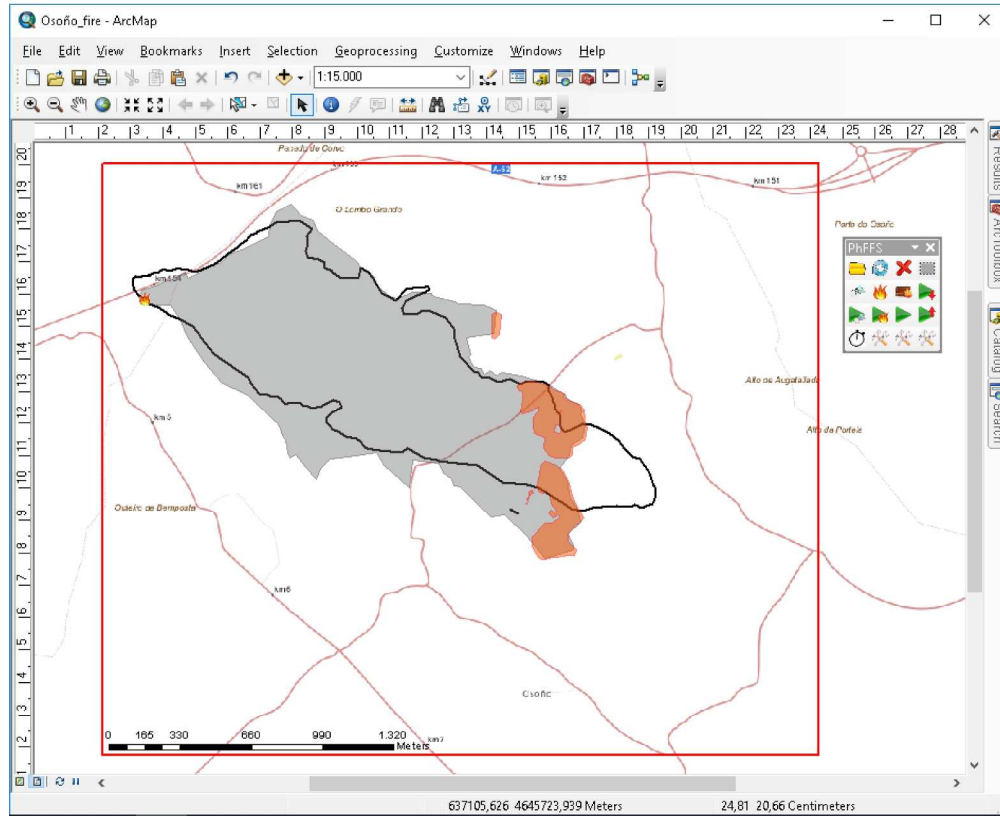


Comparison of the actual (grey) and simulated (orange) perimeter at 5.00 p.m. (a), 6.00 p.m. (b), 7.00 p.m. (c) and 8.00 p.m. (d), and the corresponding Sorensen similarity index (S), Jaccard similarity coefficient (J), and Kappa coefficient (K).

372x308mm (300 x 300 DPI)

Only

1  
2  
3  
4  
5  
6  
7  
8  
9  
10  
11  
12  
13  
14  
15  
16  
17  
18  
19  
20  
21  
22  
23  
24  
25  
26  
27  
28  
29  
30  
31  
32  
33  
34  
35  
36  
37  
38  
39  
40  
41  
42  
43  
44  
45  
46  
47  
48  
49  
50  
51  
52  
53  
54  
55  
56  
57  
58  
59  
60



Screenshot of the GIS interface displaying the actual perimeter (black line) and simulated fire: burnt area (grey) and active fire front (orange) after 3.15 hours of fire ignition (7.00 p.m.).

271x220mm (300 x 300 DPI)